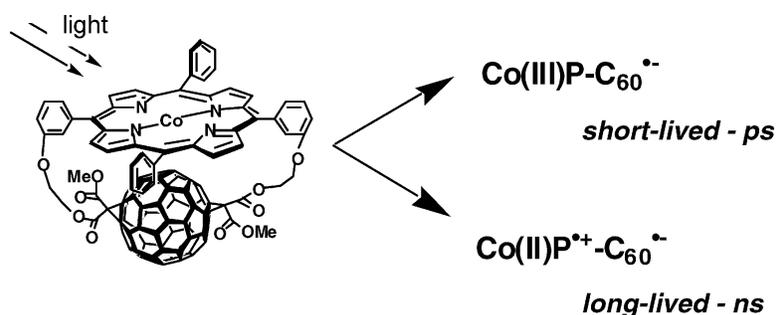## Article

Unexpected Change in Charge Transfer Behavior in a Cobalt(II) Porphyrin–Fullerene Conjugate That Stabilizes Radical Ion Pair States

Liam R. Sutton, Michael Scheloske, Kristina S. Pirner,
Andreas Hirsch, Dirk M. Guldi, and Jean-Paul Gisselbrecht

More About This Article

Additional resources and features associated with this article are available within the HTML version:

- Supporting Information
- Access to high resolution figures
- Links to articles and content related to this article
- Copyright permission to reproduce figures and/or text from this article

View the Full Text HTML

Unexpected Change in Charge Transfer Behavior in a Cobalt(II) Porphyrin−Fullerene Conjugate That Stabilizes Radical Ion Pair States

Liam R. Sutton,[†] Michael Scheloske,[†] Kristina S. Pirner,[†] Andreas Hirsch,*,[†] Dirk M. Guldi,*,[‡,+] and Jean-Paul Gisselbrecht*,[§]

Contribution from the Institut für Organische Chemie, Friedrich-Alexander-Universität Erlangen-Nürnberg, Henkestrasse 42, D-91054 Erlangen, Germany, Notre Dame Radiation Laboratory, University of Notre Dame, Notre Dame, Indiana 46556, Institute for Physical Chemistry, Friedrich-Alexander-Universität Erlangen-Nürnberg, Egerlandstrasse 3, D-91058 Erlanger, Germany, and Laboratoire d'Electrochimie et de Chimie Physique du Corps Solide, Université Louis Pasteur, UMR CNRS no. 7512, 4, rue Blaise Pascal, 67000 Strasbourg, France

Received February 23, 2004; E-mail: Dirk.M.Guldi.1@nd.edu

Abstract: Two cobalt(II) porphyrin−C_{60} malonate-linked conjugates, the mono-connected **Co1** and the bis-connected *trans*-2 isomer **Co3**, have been synthesized for the first time either by direct cyclopropanation with the precursor malonate **Co4** or by metalation of the bisadduct **H₂3**. For the investigation of the interaction between the porphyrin donor and fullerene acceptor within these dyads, electrochemical and photophysical investigations have been carried out. Compared to **Zn3** and *trans*-2 bisadduct **7**, the first reduction of the fullerene moiety within **Co3** becomes easier (40 mV in dichloromethane and 20 mV in benzonitrile), indicating significant interactions between the π-system of the fullerene and the d-orbitals of the central Co atom. Compared to the Co complexes **9**, **Co4**, and **Co1**, the first oxidation of **Co3** is considerably shifted to more positive potentials, if benzonitrile instead of dichloromethane is used as solvent. At the same time, the oxidation is no longer centered on the Co(II) center but on the porphyrin macrocycle, as corroborated by spectroelectrochemistry. A similar solvent dependence was observed in transient absorption spectroscopic measurements. In toluene, benzonitrile and anisole photoinduced electron transfer within **Co3** leads to the formation of a charge-separated state **Co(II)P•+−C₆₀•−** with a lifetime of 560 ± 20 ns in benzonitrile, whereas in other solvents such as THF, nitrobenzene, *ortho*-diclorobenzene, and *tert*-butylbenzene the formation of a **Co(III)P−C₆₀•−** as transient was detected, which is, however, short-lived (860 ± 40 ps in THF) and exhibits charge recombination dynamics that are in the Marcus inverted region. Particularly important is the fact that the electronic coupling (V) in **Co(III)P−C₆₀•−** is 18 cm^{-1} substantially smaller than the V value of 313 cm^{-1} in **ZnP•+−C₆₀•−**.

Introduction

In the photosynthetic reaction center of purple bacteria, photoinduced charge separation over a distance of several nanometers takes place by a series of electron-transfer steps between noncovalently linked porphyrin-like donors and quinone acceptors that are held together in a protein matrix.[1] A great deal of effort has been devoted to covalently linked donor and acceptor systems as photosynthetic model systems, in attempts to efficiently generate long-lived charge-separated states.[2]

Fullerenes and porphyrins are molecular architectures ideally suited for devising integrated, multicomponent model systems to transmit and process solar energy. The rich and extensive absorptions (i.e., $\pi−\pi^*$ transitions) seen in porphyrinoid systems, the pigments of life, hold particular promise for increased absorptive cross sections and, thus, an efficient use

of the solar spectrum.[3] Over the course of recent years they emanate as light harvesting building blocks in the construction of molecular architectures. Their high electronic excitation energy, typically exceeding 2.0 eV, powers a strongly exergonic electron transfer, which subsequently intercedes the conversion

[†] Institut für Organische Chemie, Friedrich-Alexander-Universität Erlangen-Nürnberg.
[‡] University of Notre Dame.
[+] Institute for Physical Chemistry, Friedrich-Alexander-Universität Erlangen-Nürnberg.
[§] Université Louis Pasteur.

(1) (a) McDermott, G.; Priece, S. M.; Freer, A. A.; Hawthornthwaite-Lawless, A. M.; Papiz, M. Z.; Cogdell, R. J.; Isaacs, N. W. *Nature* **1995**, *374*, 517. (b) Barber, J. *Nature* **1988**, *333*, 114. (c) *Supramolecular Chemistry*; Balzani, V., de Cola, L., Eds.; NATO ASI Series; Kluwer Academic Publishers: Dordrecht, The Netherlands, 1992. (d) *The Photosynthetic Reaction Center*; Deisenhofer, J., Norris, J. R., Eds.; Academic Press: New York, 1993.
(2) (a) Carter, F. L. Molecular Electronic Devices, Dekker: New York, 1987. (b) *Photoinduced Electron Transfer*; Fox, M. A., Channon, M., Eds.; Elsevier: Amsterdam, 1988. (c) *Electron Transfer in Chemistry*; Balzani, V., Ed.; Wiley-VCH: Weinheim, Germany, 2001. (d) Newton, M. D. *Chem. Rev.* **1991**, *91*, 767. (e) Wasielewski, M. R. *Chem. Rev.* **1992**, *92*, 435. (f) Gust, D.; Moore, T. A.; Moore, A. L. *Acc. Chem. Res.* **1993**, *26*, 198. (g) Paddon-Row, M. N. *Acc. Chem. Res.* **1994**, *27*, 18. (h) Gould, I. R.; Farid, S. *Acc. Chem. Res.* **1996**, *29*, 522. (i) Balzani, V.; Juris, A.; Venturi, M.; Campagna, S.; Serroni, S. *Chem. Rev.* **1996**, *96*, 759. (j) Willner, I. *Acc. Chem. Res.* **1997**, *30*, 347. (k) Piotrowiak, P. *Chem. Soc. Rev.* **1999**, *28*, 143. (k) Kurreck, H.; Huber, M. *Angew. Chem., Int. Ed. Engl.* **1995**, *34*, 849. (l) Kurreck, H.; Huber, M. *Angew. Chem.* **1995**, *107*, 929. (m) Vögtle, F. *Supramolecular Chemistry*; Wiley: Chichester, 1991. (n) Lehn, J. M. *Supramolecular Chemistry: Concepts and Perspectives*; VCH: Weinheim, Germany, 1995. (o) Steed, J. W.; Atwood, J. L. *Supramolecular Chemistry*, Wiley: Chichester, 2000.

between light and chemical and electrical energy. On the other hand, implementation of C_{60} as a three-dimensional electron acceptor holds great expectations because of their small reorganization energy in electron-transfer reactions and has exerted a noteworthy impact on the improvement of light-induced charge separation.[4] In particular, the delocalization of charges—electrons or holes—within the giant, spherical carbon framework (diameter > 7.5 Å) together with the rigid, confined structure of the aromatic π-sphere offers unique opportunities for stabilizing charged entities.[5]

The coupling of porphyrins and fullerenes is a theme of considerable current interest, given the potential applications of the photochemistry peculiar to the resulting systems in photovoltaic devices and optical limiting and molecular electronics.[6] Methods exist for synthesizing porphyrins with an almost unlimited range of functionality and regiochemistry (albeit sometimes in complex mixtures and low yield);[7] together with the emerging diversity of reliable and regioselective methods for functionalizing fullerenes,[8] the possibilities for tuning photochemical properties in such conjugates are numerous, to say the least.

Our efforts in this field have so far started with Zn(II) tetraaryl porphyrins bearing one or two malonyl esters connected via ethylene or propylene spacers to phenyl groups.[9] These compounds can then be appended to C_{60} using our modification[10] of Bingel's cyclopropanation reaction[11] at the [6,6] bonds of the fullerene to give mono- or bis-connected porphyrin−C_{60} conjugates such as **Zn1**, **Zn2**, and **Zn3** (Figure 1). Although eight distinct [6,6] bonds are in principle available for a second malonate addition, the steric requirements of the porphyrin unit tend to enforce extreme regioselectivity of bis-additions through a tether-direction effect, leading to the equatorial, *e*-isomer **Zn2** from the *cis*-porphyrin **Zn5** and *trans*-2 isomer **Zn3a** from the *trans*-porphyrin **Zn6** (Figure 1).[9f] Our photochemical investiga-

tions have revealed that excitation of the porphyrin leads to the formation of charge-separated states, which decay by charge recombination in the Marcus-inverted region.[9] This behavior is modulated by the connectivity and flexibility of the conjugates and can be further modified by the exploitation of axial metal−ligand interactions to build simple complexes or supramolecular aggregates.[9]

The impact that a redox-active metal center, such as transition metals, exerts on the stabilization of radical ion pairs in metalloporphyrin−electron acceptor conjugates is hardly ever addressed.[3] Ultrafast excited-state deactivation of the metalloporphyrin, due to efficient spin−orbit coupling, is largely responsible for this scarce. The success in probing, for example, cobalt(II) porphyrins as photoexcited state electron donors depends on overcoming the fast excited state deactivation. An obvious strategy mandates an intramolecular charge separation event that is substantially fast. Considering that the thermodynamics for charge separation in porphyrin−fullerene conjugates are in the top region of the Marcus parabola, the effective rate constant remains a function of the electronic coupling matrix. The unique topology in the **3a** series ensures strong coupling with values that peak around 436 cm^{-1}, which consequently leads to rate constants faster than 10^{12} s^{-1}.[9f]

We report here the synthesis of Co(II)-containing analogues of **Zn1** and **Zn3**, namely **Co1** and **Co3**, as novel photosynthetic model systems. A major incentive for probing cobalt porphyrins stems from their enzymatic catalytic reactivity, such as the function of coenzyme B$_{12}$.[12] We then present our observations of the photochemical and redox behavior of the resulting compounds in comparison with a number of model molecules, showing that alteration of the metal contained within the porphyrin has a profound effect on the physicochemical properties of porphyrin−fullerene conjugates. Most outstandingly, depending on the nature of the oxidation, that is, metal- versus ligand-centered process, charge recombination can be suppressed by up to *3 orders of magnitude*.

Results and Discussion

Syntheses. We chose to synthesize our Co(II) porphyrin−fullerene adducts either via the Zn(II) analogues, demetalation, and Co(II) insertion or via direct coupling of a Co(II)-containing porphyrin with C_{60}, taking into account a number of factors: (a) the free base intermediates represent a useful target in their own right, for examination of physical properties and as a starting point for the insertion of a wide range of metal cations, (b) Bingel additions of metalated porphyrins to fullerenes proceed in higher yield than those of free base porphyrins, (c) demetalation of the Zn(II) adducts was expected to be straightforward and proved to be so, (d) Co(II) is paramagnetic, presenting characterization difficulties when using it in intermediate stages, and (e) the direct route is the least complicated.

Free base porphyrins **H$_2$4**, **H$_2$5**, and **H$_2$6** were synthesized by the statistical condensation of 2 equiv of pyrrole, 1 equiv of benzaldehyde, and 1 equiv of malonyl-substituted benzaldehyde under high dilution conditions (ca. 0.1 M benzaldehyde) under various well-established sets of conditions, followed by oxidation with excess 2,3-dichloro-5,6-dicyano-1,4-diquinone (DDQ)

(3) *The Porphyrin Handbook*; Kadish, K. M., Smith, K. M., Guilard, R., Eds.; Academic Press: New York, 1999.
(4) For recent reviews on fullerene-containing donor−acceptor ensembles and fullerene anions, see: (a) Imahori, H.; Sakata, Y. *Adv. Mater.* **1997**, *9*, 537. (b) Prato, M. *J. Mater. Chem.* **1997**, *7*, 1097. (c) Martin, N.; Sanchez, L.; Illescas, B.; Perez, I. *Chem. Rev.* **1998**, *98*, 2527. (d) Imahori, H.; Sakata, Y. *Eur. J. Org. Chem.* **1999**, 2445. (e) Guldi, D. M. *Chem. Commun.* **2000**, 321. (f) Guldi, D. M.; Prato, M. *Acc. Chem. Res.* **2000**, *33*, 695. (g) Reed, C. A.; Bolskar, R. D. *Chem. Rev.* **2000**, *100*, 1075. (h) Gust, D.; Moore, T. A.; Moore, A. L. *J. Photochem. Photobiol., B* **2000**, *58*, 63. (i) Gust, D.; Moore, T. A.; Moore, A. L. *Acc. Chem. Res.* **2001**, *34*, 40. (j) Guldi, D. M.; Martin, N. *J. Mater. Chem.* **2002**, 1978−1992.
(5) (a) Guldi, D. M.; Neta, P.; Asmus, K.-D. *J. Phys. Chem.* **1994**, *98*, 4617. (b) Guldi, D. M.; Asmus, K.-D. *J. Am. Chem. Soc.* **1997**, *119*, 5744. (c) Imahori, H.; Hagiwara, K.; Akiyama, T.; Aoki, M.; Taniguchi, S.; Okada, T.; Shirakawa, M.; Sakata, Y. *Chem. Phys. Lett.* **1996**, *263*, 545.
(6) (a) Fukuzumi, S.; Guldi, D. M. *Electron Transfer in Chemistry* **2001**, *2*, 270−337. (b) Imahori, H.; Guldi, D. M.; Tamaki, K.; Yoshida, Y.; Luo, C.; Sakata, Y.; Fukuzumi, S. *J. Am. Chem. Soc.* **2001**, *123*, 6617−6628. (c) Guldi, D. M. *Chem. Soc. Rev.* **2002**, *31*, 22−36.
(7) *The Porphyrin Handbook*; Kadish, K. M., Smith, K. M., Guilard, R., Eds.; Academic Press: San Diego, CA, 2000; Volume 1: Synthesis and Organic Chemistry, and Volume 2: Heteroporphyrins, Expanded Porphyrins and Related Macrocycles.
(8) (a) Hirsch, A. *Top. Curr. Chem.* **1999**, *199*, 1−65. (b) Diederich, F.; Kessinger, R. *Acc. Chem. Res.* **1999**, *32*, 537−545. (c) Diederich, F.; Kessinger, R. *Templated Org. Synth.* **2000**, 189−218.
(9) (a) Dietel, E.; Hirsch, A.; Eichhorn, E.; Rieker, A.; Hackbarth, S.; Roder, B. *Chem. Commun.* **1998**, 1981−1982. (b) Dietel, E.; Hirsch, A.; Zhou, J.; Rieker, A. *J. Chem. Soc., Perkin Trans. 2* **1998**, 1357−1364. (c) Camps, X.; Dietel, E.; Hirsch, A.; Pyo, S.; Echegoyen, L.; Hackbarth, S.; Roder, B. *Chem.−Eur. J.* **1999**, *5*, 2362−2373. (d) Guldi, D. M.; Luo, C.; Da Ros, T.; Prato, M.; Dietel, E.; Hirsch, A. *Chem. Commun.* **2000**, 375−376. (e) Guldi, D. M.; Luo, C.; Prato, M.; Dietel, E.; Hirsch, A. *Chem. Commun.* **2000**, 373−374. (f) Guldi, D. M.; Luo, C.; Prato, M.; Troisi, A.; Zerbetto, F.; Scheloske, M.; Dietel, E.; Bauer, W.; Hirsch, A. *J. Am. Chem. Soc.* **2001**, *123*, 9166−9167.
(10) Camps, X.; Hirsch, A. *J. Chem. Soc., Perkin Trans. 1* **1997**, 1595−1596.
(11) Bingel, C. *Chem. Ber.* **1993**, *126*, 1957−1959.
(12) (a) Anson, F. C.; Shi, C.; Steiger, B. *Acc. Chem. Res.* **1997**, *30*, 437. (b) Collman, J. P.; Wagenknecht, P. S.; Hutchison, J. E. *Angew. Chem., Int. Ed. Engl.* **1994**, *53*, 1537. (c) Frey, P. *Chem. Rev.* **1990**, *90*, 1343. (d) Buckel, W.; Golding, B. T. *Chem. Soc. Rev.* **1996**, *25*, 329.
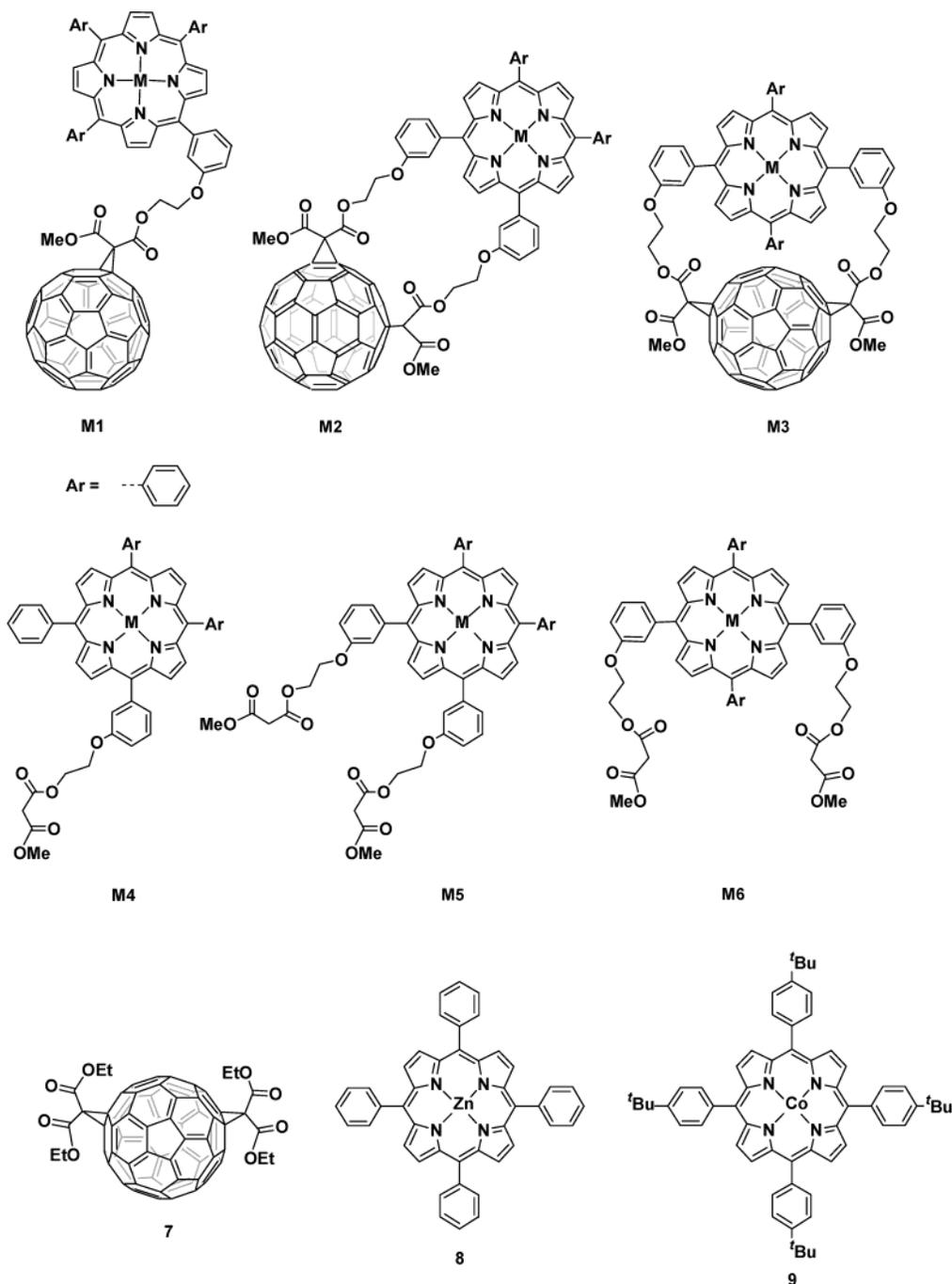
Figure 1. Porphyrin−fullerene adducts. M = H₂, Zn, or Co.

or *p*-chloranil. The reaction mixture was concentrated, and excess methanol was added to precipitate the porphyrins. The precipitate was obtained by vacuum filtration, and the individual porphyrins were isolated by column chromatography on silica gel with 5 v/v % EtOAc in dichloromethane as eluent and recrystallization by addition of MeOH to concentrated dichloromethane solutions of the appropriate bands. Yields were statistical and reasonable, at around (in order of increasing retention time) 5% for **H₂4**, 2% **H₂6**, and 4% **H₂5**, giving quantities of the order of 100−1000 mg of porphyrin per reaction.

Zn(II) was then conveniently inserted into the free base porphyrins using excess Zn(OAc)₂ in CH₂Cl₂/MeOH mixtures,

with yields that were almost quantitative. Co(II) could alternatively be inserted at this stage by the use of Co(OAc)₂ in refluxing THF over 6 h.

Using the modified Bingel reaction,[10] we were able to effect the mono- and bis-additions in good yield. The bis-addition can be regarded as macrocyclization; high dilution of the reagents (1:1 C₆₀/porphyrin, DBU, and I₂ in toluene), stirring at room temperature for 16 h, and purification by chromatography resulted in yields of around 50% **Zn3** (see also ref 9).

Zn(II) was quantitatively removed from the adducts **Zn1** and **Zn3** by treatment of 25-mL toluene solutions with excess 3:1 v/v TFA/MeOH. Addition of acid resulted in the immediate formation of dark green solutions, which after stirring at room
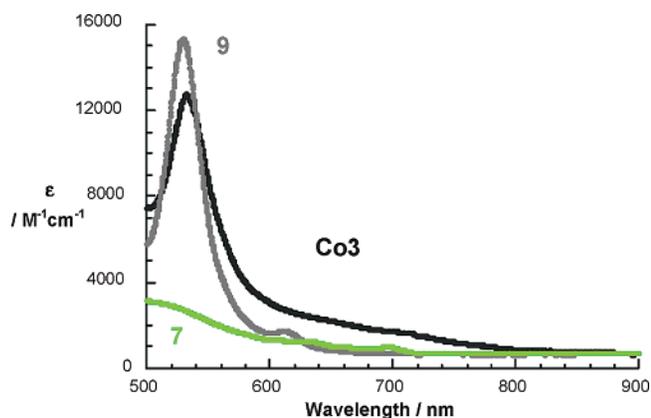
Figure 2. Absorption spectra of CoT*t*-BuPP (**9**), **Co3**, and *trans*-2−C$_{62}$-(COOEt)$_4$ (**7**) in toluene.

temperature for 15 min were washed with 4 × 25 mL of H$_2$O, resulting in dark purple-brown color in the organic phase. Evaporation of the organic solvent and drying in vacuo gave the free base adducts **H$_2$1** and **H$_2$3**.

The monoadduct **Co1** was obtained by direct cyclopropanation of C$_{60}$ with **Co4**. Co(II) was inserted into **H$_2$3** by the action of excess Co(OAc)$_2$ in THF under reflux. The progress of the reaction was monitored by TLC, although differences in R_f values of free base and Co(II) adducts were small. The metalated **Co3** was formed rather more slowly: 24 h were required before all of the starting material was consumed, presumably because one face of the porphyrin was completely blocked by fullerene. **Co1** and **Co3** were purified by column chromatography or filtration through a silica gel plug followed by recrystallization. The resulting compounds were pure by TLC, and microanalysis and mass spectrometry revealed molecular ion peaks. NMR was, however, complicated by the paramagnetism of d^7 Co(II): ^{1}H spectra were downfield-shifted and broadened, most markedly those peaks corresponding to protons nearest to the metal center.

Absorption Characteristics. The ground-state absorption spectra of the investigated conjugates **Co1** and **Co3** are indicative of the divalent cobalt oxidation state. In particular, the maxima around 535 nm are good matches to a cobalt(II) porphyrin reference (CoT*t*-BuPP (**9**)) lacking a **C$_{60}$** moiety. This supports the view that linking a strong electron acceptor, such as C$_{60}$, to the cobalt(II) porphyrin has no direct effect on the cobalt's oxidation state. However, the close proximity of the porphyrin and fullerene π-systems gives rise to through-space interactions, whose effects lead to red-shifts of the *Soret* and *Q*-band transitions. In the 700−800 nm region (see Figure 2), the spectra of **Co1** and **Co3** reveal a new broad band, which we assign to a charge-transfer transition between the porphyrin donor and the electron accepting fullerene. The presence of the additional band therefore confirms electronic interaction between the two chromophores in the dyads.

Electrochemical and Spectroelectrochemical Investigations. Electrochemical investigations−cyclic voltammetry (CV) and rotating disk voltammetry (RDV)−were carried out in benzonitrile and dichloromethane containing 0.1 M Bu$_4$NPF$_6$ as supporting electrolyte. With the help of the corresponding building blocks, namely, *trans*-2−C$_{62}$(COOEt)$_4$ (**7**),[13] ZnTPP (**8**), and CoT*t*-BuPP (**9**), which were studied as reference

Table 1. Redox Potentials Observed in CH$_2$Cl$_2$ + 0.1 M Bu$_4$NPF$_6$ on a Glassy Carbon Working Electrode by Cyclic Voltammetry at a Sweep Rate of 0.1 Vs^{-1}

	Potentials in Volts vs Fc$^+$/Fc^a						
compd	$E_{Red4}'°$	$E_{Red3}'°$	$E_{Red2}'°$	$E_{Red1}'°$	$E_{Ox1}'°$	$E_{Ox2}'°$	$E_{Ox3}'°$
7	−2.30	−1.95 ^{b}	−1.40	−1.05			
8				−1.80	+0.34	+0.65	
9				−1.35	+0.28	+0.53	+0.79
Co4			−1.80^b	−1.34	+0.35	+0.60	+0.85
Zn3	−2.05^b	−1.90^c	−1.51	−1.10	+0.34	+0.69	
Co1			−1.42 (2 e$^-$)	−0.99	+0.37	+0.61	+0.85
Co3		−1.78^b	−1.57 (2 e$^-$)	−1.01	+0.40	+0.82	+0.96

^{a} Formal redox potential $E'° = (E_{pa} + E_{pc})/2$. ^{b} Peak potentials for irreversible electron transfers. ^{c} Quasi reversible electron exchange: ΔE_p =120 mV at $v = 0.1$ V/s.

compounds under the same experimental conditions, the redox behavior of the zinc(II) and cobalt(II) porphyrin−fullerene conjugates was interpreted. All redox potentials are summarized in Tables 1 and 2.

Electrochemical Investigation of Zn3. In benzonitrile, the cyclic voltammetry (CV) of **Zn3** (Figure 3) gives rise to three well-resolved one-electron oxidation processes. The reversibility of these processes was examined by testing their peak currents (I_p) and peak potentials (E_p) at variable scan rates (v). Importantly, the corresponding peak potentials are constant up to scan rates of 2 V/s, while the peak current ratio I_{pa}/I_{pc} is close to unity at any v. The peak potential difference, that is, $\Delta E_p = E_{pc} − E_{pa}$ always remains close to 57 mV (i.e., up to 1 V/s), and the I_p vs $v^{1/2}$ relationship shows a linear correlation with an intercept that cuts through the origin.

On the reduction side, a series of reduction steps were developed. Clearly, the first reduction is a one-electron reversible transfer, as suggested by the peak characteristics evolution with scan rates. The second reduction behaves as an irreversible electron transfer at sweep rates lower than 0.1 V/s. At sweep rates exceeding 1 V/s, the electron transfer becomes, however, reversible. The evolution of the peak characteristics is in agreement with an EC$_{irrev}$ mechanism, namely, a reversible electron transfer followed by an irreversible chemical reaction. Two additional reduction steps were observed at, respectively, −1.82 and −2.03 V, which revealed characteristics of either quasi-reversible or reversible electron-transfer processes.

In dichloromethane, only two one-electron reversible oxidations were observed, while the third one was masked by the electrolyte discharge. The first and second reductions have characteristics of a reversible one-electron step for sweep rates above 0.5 V/s, whereas at sweep rates below 0.5 V/s the second reduction exhibits a trend toward irreversibility. Overall, the redox behavior is similar in both solvents.

A closer inspection of Table 1 and a comparison with the individual reference compounds leads to the following conclusions: The redox behavior of **Zn3** comprises first and second oxidation processes that occur on the zinc porphyrin, while a third oxidation, only observed in benzonitrile, removes an electron from the C$_{60}$ core. On the other hand, the two first reduction processes correspond to the formation of radical anion and dianion of the fullerene. Because of the instability of the dianion, as commonly observed for C$_{60}$ bisadducts,[14] several

(13) Hirsch, A.; Lamparth, I.; Karfunkel, H. R. *Angew. Chem.* **1994**, *106*, 453− 455; *Angew. Chem., Int. Ed. Engl.* **1994**, *33*, 437−439.

(14) Kessinger, R.; Gomez-Lopez, M.; Boudon, C.; Gisselbrecht, J. P.; Gross, M.; Echegoyen, L.; Diederich, F. *J. Am. Chem. Soc.* **1998**, *120*, 8545− 8546.

Table 2. Redox Potentials Observed in PhCN + 0.1 M Bu$_4$NPF$_6$ on a Platinum Working Electrode by Cyclic Voltammetry at $v = 0.1$ Vs^{-1}

compd	Potentials in Volts vs Fc$^+$/Fc[a]							
	$E_{Red4}'^\circ$	$E_{Red3}'^\circ$	$E_{Red2}'^\circ$	$E_{Red1}'^\circ$	$E_{Ox1}'^\circ$	$E_{Ox2}'^\circ$	$E_{Ox3}'^\circ$	$E_{Ox4}'^\circ$
7	−2.06	−1.91[b]	−1.36	−0.95	+1.21	+1.56[b]		
8			−2.20	−1.80	+0.35	+0.75		
9				−1.35	0.0	+0.67	+0.95	
Co4				−1.34	E_{pa} = +0.09	+0.71	+0.99	
					E_{pc} = −0.21			
Zn3	−2.03	−1.82	−1.40	−1.02	+0.37	+0.77	+1.26	
Co1	−2.12	−1.92[b]	−1.41 (2 e$^-$)	−0.92	+0.06	+0.72	+0.98	+1.22
Co3	−1.90[c]	−1.77[c]	−1.50[d]	−0.93	+0.28	+0.78	+1.03	+1.27

[a] Formal redox potential $E'^\circ = (E_{pa} + E_{pc})/2$. [b] Peak potentials for irreversible electron transfers. [c] Small amplitude not well resolved steps. [d] Two overlapping one-electron reductions separated by 60 mV.
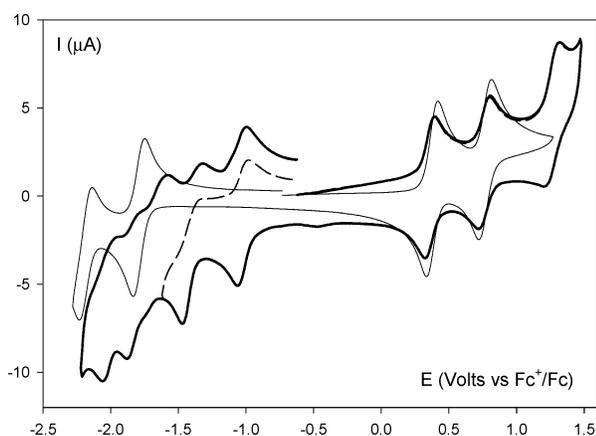

Figure 3. Cyclic voltammetry ($v = 0.1$V/s) of ZnTPP and **Zn3** in PhCN + 0.1 M Bu$_4$NPF$_6$. Hair line: CV of ZnTPP (**8**); bold line: CV of **Zn3**; dashed line: CV of **Zn3**, reverting the scan at −1.6 V.

electrogenerated electroactive species are present in solution. This complication renders the assignment of the reduction processes in the more negative region virtually impossible.[15]

Electrochemical Investigation of Co1a and Co3a. Five oxidation steps were noted in cyclic voltammetric experiments with **Co1** and **Co3** in benzonitrile (Figures 4 and 5). The first oxidation is quasi-reversible, since the peak separation ΔE_p (i.e., $E_{pc} - E_{pa}$) varied with scan rate. Commonly, this process is assigned to a metal-centered redox oxidation, that is, formation of Co(III).[16] The quasi-reversible behavior is not entirely unexpected because of changes in the axial coordination, which are likely to occur during the metal oxidation. Steps two and three correspond to reversible one-electron oxidations of the macrocyclic ligand. On the contrary, the fourth and fifth one-electron oxidations involve the C$_{60}$ moiety.[17,18]

Two well-defined reversible reduction steps were observed on the reductive side. Whereas the first reduction involves just a one-electron transfer, the second reduction implicates a

(15) The resulting CV is not a simple addition of the CVs of **7** and **8**, because of site−site interactions and Coulombic repulsions between highly reduced species.
(16) (a) Truxillo, L. A.; Davis, D. G. *Anal. Chem.* **1975**, *47*, 2260−2267. (b) Kadish, K. M. In *Progress in Inorganic Chemistry*; Lippard, S. J., Ed.; Wiley & Sons: New York, 1986; Vol. 34, p 443. (c) Kadish, K. M.; Lin, X. Q.; Han, B. C. *Inorg. Chem.* **1987**, *26*, 4161−4167. (d) Lin, X. Q.; Boisselier-Cocolios, B.; Kadish, K. M. *Inorg. Chem.* **1986**, *25*, 3242−3248. (e) Huet, D.; Gaudemer, A.; Boucly-Goester, C.; Boucly, P. *Inorg. Chem.* **1982**, *21*, 3413−3419.
(17) (a) Cardullo, F.; Seiler, P.; Isaacs, L.; Nierengarten, J. F.; Haldimann, R. F.; Diederich, F. *Helv. Chim. Acta* **1997**, *80*, 343−371. (b) Nierengarten, J. F.; Habicher, T.; Kessinger, R.; Cardullo, F.; Diederich, F.; Gramlich, V.; Gisselbrecht, J. P.; Boudon, C.; Gross, M. *Helv. Chim. Acta* **1997**, *80*, 2238−2276.
(18) Guarr, T. F.; Meier, M. S.; Vance, V. K.; Clayton, M. *J. Am. Chem. Soc.* **1993**, *115*, 9862−9863.
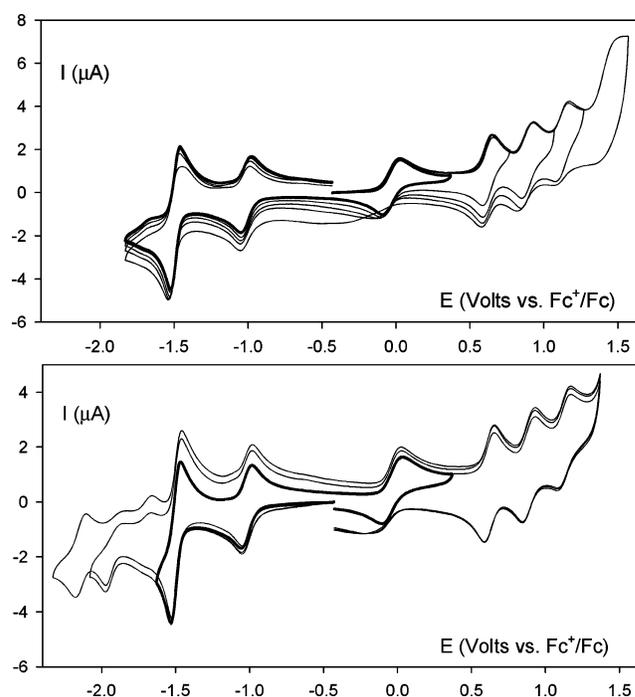

Figure 4. Cyclic voltammetry ($v = 0.1$ V/s) of **Co1** in benzonitrile and 0.1 M Bu$_4$NPF$_6$ for different anodic (top) or cathodic (bottom) switching potentials.
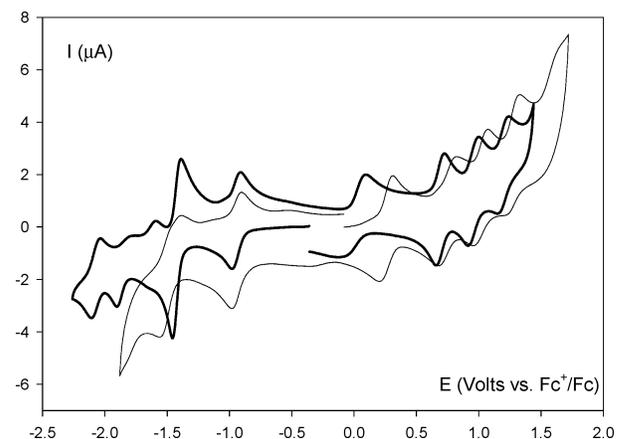

Figure 5. Cyclic voltammetry ($v = 0.1$ V/s) of **Co1** (bold line) and **Co3** (hair line) in benzonitrile and 0.1 M Bu$_4$NPF$_6$.

sequence of two electrons. The characteristics of the latter electron exchange depend, however, on the conjugate. For **Co1** the peak potential difference is close to 57 mV, with a peak current approximately twice what is seen for the first reduction peak. It is important to note that the peak shape reveals

characteristics of two overlapping one-electron transfers, occurring, however, at nearly identical potentials. The formal redox potential difference between the two one-electron transfers is close to 37 mV, which corroborates the existence of two independent redox centers.[19] In **Co3** the two overlapping reductions are separated by 60 mV. Comparison with the redox potentials of the precursors clearly indicates that the two overlapping reduction steps in **Co3** involve the one-electron reduction of the C_{60} moiety and the first one-electron reduction of the cobalt porphyrin moiety.[20]

The CVs in dichloromethane are similar to those described for benzonitrile as a solvent. However, because of interferences with the electrolyte discharge the number of reduction and oxidation processes is restricted. In particular, only the first three oxidations, all involving the cobalt porphyrin moiety, were observed. On the reductive side, only two reduction steps were registered. Again, the second step implicates two overlapping one-electron steps, one occurring at the C_{60} moiety and one at the CoP moiety.

To summarize, the studied porphyrin–fullerene conjugates clearly show that the resulting CVs are not just the simple addition of the CVs of the two reference building blocks. The observed differences are due to "site–site" interactions. When comparing **Zn3** and **Co3** with *trans*-2–$C_{62}(COOEt)_4$ (**7**), the first fullerene reduction in **Zn3** renders more difficult in both solvents (dichloromethane: 50 mV; benzonitrile: 70 mV), whereas for **Co3**, the first reduction of C_{60} becomes easier (dichloromethane: 40 mV; benzonitrile: 20 mV). Such a potential shift to more positive potentials may result from electrostatic interactions in **Co3**. Indeed, similar potential shifts have been observed for fullerene–dibenzo[18]crown-6 conjugates in the presence of potassium salts.[21]

Spectroelectrochemical Investigations. To identify the electron-transfer sites for the CoT*t*-BuPP (**9**) and **Co3**, the electrochemical studies were complemented by spectroelectrochemical investigations in dichloromethane and in benzonitrile. In dichloromethane, **9** and **Co3** give rise to similar spectral evolutions during the first oxidation step. On the basis of the literature, we assigned these data to a metal-centered electron transfer.[16]

Figure 6 illustrates that the spectroelectrochemistry performed in benzonitrile leads for **9** and **Co3** to different spectral evolutions. During the first oxidation of **9** the initial bands at 418 and 532 nm disappeared, while new bands appeared at 442, 555, and 592 nm. These spectral features are characteristics of a Co(III) complex and are in agreement with previous data observed in the same solvent by Wolberg.[22] The spectrum registered after the completion of the second oxidation with maxima at 426, 439(sh), 647, 740, 846, and 941 nm is that of a radical cation.

For **Co3**, the initial bands at 423 and 533 nm vanished during the electrolysis performed at the plateau potential of the first oxidation. Simultaneously, new bands at 391, 443, and 559 nm developed. The drastic differences, relative to **9**, are seen mainly
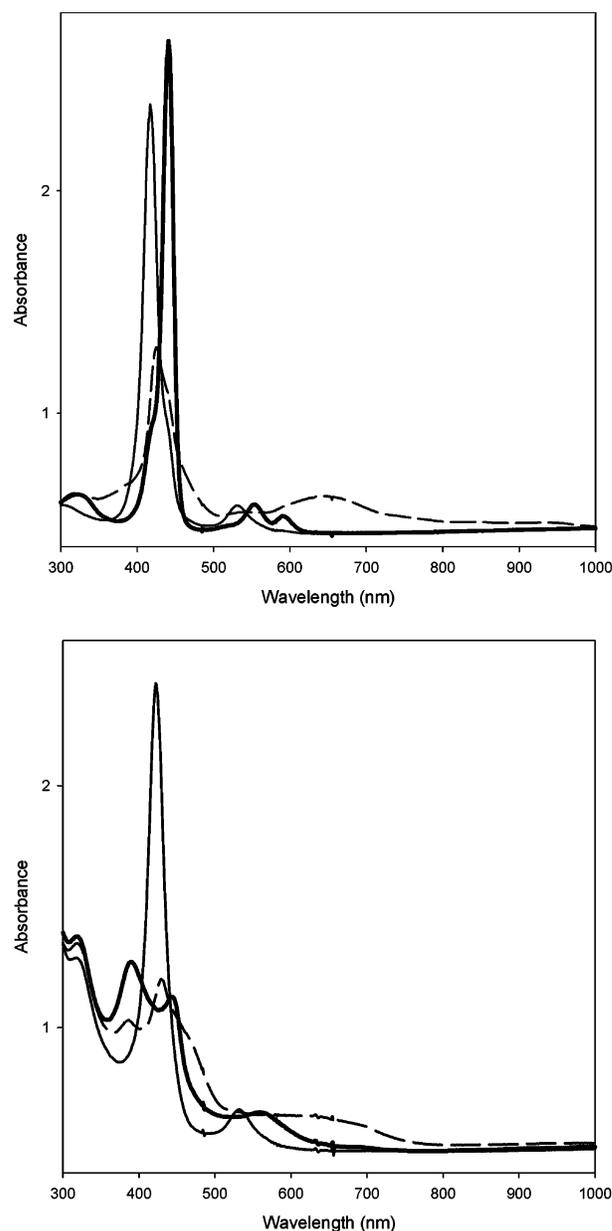
(19) (a) Flanagan, J. B.; Margel, S.; Bard, A. J.; Anson, F. C. *J. Am. Chem. Soc.* **1978**, *100*, 4248–4253. (b) Ammar, F.; Savéant, J. M. *J. Electroanal. Chem.* **1973**, *47*, 215–221.
(20) Further reductions are not well resolved for **Co3a** (Figure 5), whereas for **Co1a** two further reductions are observed as shown in Figure 4.
(21) Bourgeois, J. P.; Seiler, P.; Fibbioli, M.; Pretsch, E.; Diederich, F.; Echegoyen, L. *Helv. Chim. Acta* **1999**, *82*, 1572–1595.
(22) Wolberg, A.; Manassen, J. *J. Am. Chem. Soc.* **1970**, *92*, 2982–2991.

Figure 6. Spectra of the cobalt(II) species (line), the one-electron oxidized species (bold line), and the two one-electron oxidized species (dashed line) obtained during spectroelectrochemical oxidation of **9** (upper) and **Co3** (lower) in benzonitrile and 0.1M Bu₄NPF₆.

in the large decrease of the Soret band. Tentatively, we assigned this process to the generation of the corresponding radical cation **Co3•+**. Additional support for our hypotheses was borrowed from previous observations related to the radical cations of CuOETPP[23] and (Im)₂NiOETPP.[24] The drastic spectral differences observed during the first oxidation step of the cobalt porphyrin **Co3** in benzonitrile indicate the generation of the radical cation and not that of the cobalt(III) species, since the Co(III) spectral characteristics were not observed at all. Oxidation at the plateau potential of the second oxidation step, which corresponds to an overall exchange of two electrons, yielded a spectrum whose characteristics (i.e., maxima at 388, 432,

(23) Renner, M. W.; Barkigia, K. M.; Zhang, Y.; Medforth, C. J.; Smith, K. M.; Fajer, J. *J. Am. Chem. Soc.* **1994**, *116*, 8582–8592.
(24) Renner, M. W.; Barkigia, K. M.; Melamed, D.; Gisselbrecht, J. P.; Nelson, N. Y.; Smith, K. M.; Fajer, J. *Res. Chem. Intermed.* **2002**, *28*, 741–759.

466(sh), 630, and 694 nm) are typical of a dicationic species. It has to be mentioned that for **9** and **Co3**, the initial spectra could be recovered quantitatively by stepwise reduction of the generated dicationic species.

In conclusion, despite the similar electrochemical behavior for **9** and **Co3** in benzonitrile, the spectroelectrochemical investigations clearly indicate that the oxidation of **Co3** corresponds to the following mechanism:

$$\textbf{Co(II)P} \rightarrow \textbf{Co(II)P}^{\bullet+} + e^-;$$
$$\textbf{Co(II)P}^{\bullet+} \rightarrow \textbf{Co(III)P}^{2+} + e^-$$
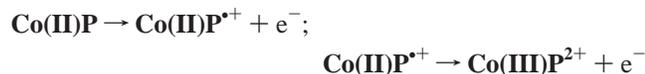
whereas for **9**, the first one-electron oxidation generates the expected cobalt(III) complex

$$\textbf{Co(II)P} \rightarrow \textbf{Co(III)P}^+ + e^-$$

Photophysical Investigations. Because of the paramagnetism of the $3d^7$ electronic configuration, the excited states of cobalt(II) porphyrin are rapidly deactivated. Despite the low-spin character ($s = 1/2$) of **CoP**, the good overlap between the transition metal d orbitals and the macrocyclic lone pairs is responsible for directing the deactivation from the metal center to the porphyrin's $\pi-\pi^*$ transitions. The emission spectra reveal an eminent impact of the strong deactivation. In room-temperature experiments, neither fluorescence nor phosphorescence was seen, in contrast to the high fluorescence quantum yields ($\Phi = 0.11$) of the free base porphyrin (**H₂P**) analogue.[25] The fact that even phosphorescence is abolished prompts us to the fact that all possible excited states are equally rapid deactivated. In summary, the fast excited-state deactivation of cobalt(II) porphyrin prevents assessing the charge separation kinetics on the basis of fluorescence spectroscopy. Likewise, time-resolved fluorescence decay measurements failed to indicate any noteworthy emission.

Similar to the spectrum of **CoP−C₆₀** (i.e., **Co1** and **Co3**), no notable light emission was recorded in the 550−1000 nm region. Please note that the analogous zinc (**Zn3**) and free base conjugates (**H₂3**) both give rise to emissive charge-transfer features with quantum yields as high as 10^{-3} in the free base case. The lack of appreciable charge-transfer emission, especially for **Co3**, is observed in several solvents with a wide range of polarity (i.e., toluene, THF, and benzonitrile).

Considering the electrochemical analysis of **Co1** and **Co3** in dichloromethane and benzonitrile, we estimated the energy for the charge-separated state, that is, a one-electron oxidized porphyrin and a one-electron reduced fullerene, to be around 1.4 and 1.3 eV, respectively. The lack of emissive features hampers, however, the exact determination of the excited-state energies. The long wavelength absorption in the ground-state spectrum, which reflects the vertical up transition across the ground state−singlet excited state energy gap, at ∼535 nm allows us to deduce only an upper limit of the singlet excited state (∼2.0 eV). Further support for this energetic positioning can be lent from the data established for the analogous zinc and free base porphyrins, which are at ∼2.0 eV (singlet excited state) and ∼1.5 eV (triplet excited state).[26] Thus, under strict

(25) Murov, S. L.; Carmichael, I.; Hug, G. L. *Handbook of Photochemistry*; Marcel Dekker: New York, 1993.
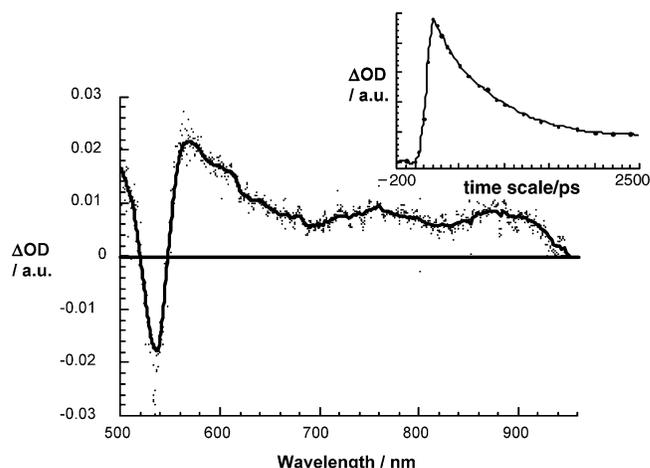(26) Luo, C.; Guldi, D. M.; Imahori, H.; Tamaki, K.; Sakata, Y. *J. Am. Chem. Soc.* **2000**, *122*, 6535.

Figure 7. Picosecond transient absorption spectrum (visible−near-infrared part) recorded with a 100 ps upon flash photolysis of dyad **Co3** (∼5.0 × 10^{-5} M) at 532 nm in deoxygenated THF, indicating the Co(III)P features (λ_{max} = 560 and 590 nm) and C₆₀ π-radical anion features (λ_{max} = 900 nm) − Co(III)P−C₆₀•⁻. Insert depicts the decay of the Co(III)P features at 560 nm.

thermodynamic considerations and neglecting the short-lived nature of photoexcited **CoP** (see below) a photoinduced electron transfer evolving between the excited electron donating cobalt(II) porphyrins and C₆₀ as the electron acceptor is energetically feasible.

To probe and visualize the electron transfer in photoexcited **Co1** and **Co3**, we performed time-resolved transient absorption spectroscopy following short laser excitation (i.e., 18 ps or 8 ns) of the porphyrin chromophore at 532 nm. For the reference **9**, we monitored in picosecond pump−probe experiments a very short-lived transient. Spectroscopic features of this intermediate in the 500−760 nm range are transient bleaching at 530 nm flanked by new maxima at 500 and 555 nm. The lifetime is very short and our ∼18 ps time resolution only allows an upper limit estimation of ca. 30 ps. This value is in satisfying agreement with previous reports.[27] It should be pointed out that the new spectrum disappeared completely about 50 ps after the pulse. Also, no residual transient features were registered on the micro- and millisecond time scale.

The transient absorption changes associated with **Co3** in THF are drastically different. The 500−960 nm region is depicted in Figure 7. For comparison, we have added the transient seen for the zinc conjugate **Zn3** in Figure S1. Immediately after the picosecond pulse a transient species is seen that displays a set of maxima at 560 and 590 nm. Both features resemble the characteristics of a square-planar $3d^6$ configuration found upon metal-center oxidation of cobalt(II) porphyrin by electrochemical[22] and pulse radiolytical means.[28] This is in sharp contrast to the ligand-centered oxidation process, which was observed earlier for **Zn3** and free base analogues. Further in the red, around 900 nm, a maximum is seen that resembles C₆₀•⁻ seen in a typical *trans*-2 adduct such as **7**. Thus, we conclude that the energetically low-lying radical pair is constituted by a **Co-(III)P−C₆₀•⁻** state as a product of an ultrafast photoinduced electron transfer. The formation is buried within our experimental time resolution, that is, <18 ps. To shed light onto the electron-transfer kinetics in **Co3**, the zinc conjugate **Zn3** proved

(27) Rodriguez, J.; Kirmaier, C.; Holton, D. *J. Am. Chem. Soc.* **1989**, *111*, 6500.
(28) Neta, P.; Grebel, V.; Levanon, H. *J. Phys. Chem.* **1981**, *85*, 2117.
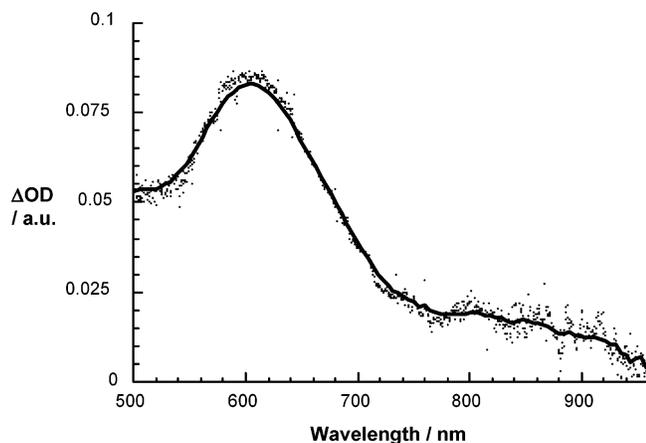
Figure 8. Picosecond transient absorption spectrum (visible−near-infrared part) recorded with a 100 ps upon flash photolysis of dyad **Co3** (∼5.0 × 10^{-5} M) at 532 nm in deoxygenated benzonitrile, indicating the Co(II)P π-radical cation features (λ_{max} = 600 nm) − Co(II)P$^{\bullet+}$.

to be helpful. Most importantly, the redox features of **Zn3** and **Co3** are in close resemblance and ensure similar thermodynamic driving forces. Steady-state fluorescence experiments suggest that in **Zn3** the electron transfer occurs with lower to subpicosecond rates and, thus, sufficiently fast to compete with the intrinsic deactivation of the cobalt(II) porphyrin in **Co3** (i.e., less than 30 ps).[12]

Both fingerprints (i.e., ∼560 and 900 nm) were employed as reliable probes to determine the lifetime of the associated **Co(III)P−C$_{60}$$^{\bullet-}$** state in **Co3**. The decay curves were well-fitted by a single exponential decay component. In particular, lifetimes that are 860 ± 40 ps were derived from the decays of the oxidized donor and reduced acceptor absorption at 560 and 900 nm, respectively.

In benzonitrile, the photoreactivity of **Co3** changed drastically. At a time delay, when the **Co(III)P−C$_{60}$$^{\bullet-}$** maxima were recorded in THF, the rather sharp transient of cobalt(III) porphyrin is replaced by a very broad absorption that covers most of the 500−750 nm range and exhibits a maximum at 600 nm. In fact, the spectrum as shown in Figure 8 bears close resemblance with a one-electron oxidized ligand product, π-radical cation. Around 900 nm, we found the characteristic fingerprint of the fullerene π-radical anion. Thus, the spectroscopic analysis suggests formation of a **Co(II)P$^{\bullet+}$−C$_{60}$$^{\bullet-}$** radical pair, contrasting the observation in THF. The decay of the **Co(II)P$^{\bullet+}$−C$_{60}$$^{\bullet-}$** radical pair, at 600 (**Co(II)P$^{\bullet+}$**) and 900 nm (**C$_{60}$$^{\bullet-}$**), is best fitted by a monoexponential rate law, from which we derive a lifetime for the radical pair of 560 ± 20 ns (!) in benzonitrile.

The difference in electron-transfer reactivity, that is, involvement of either **Co(II)P$^{\bullet+}$**, which brings about a very long-lived radical pair, or **Co(III)P** and a short-lived radical pair, raises the question about the factors that are responsible for these effects. It should be noted that both solvents are coordinating ones that might interact with the free axial ligand sphere of the cobalt(II), but have substantially different polarity. Thus, we probed DMF, another coordinating solvent, whose polarity is close to that of benzonitrile. Surprisingly, the product of the photoinduced charge-transfer event is again the short-lived (0.15 ns) **Co(III)P−C$_{60}$$^{\bullet-}$** state. This rules out the solvent polarity effect and also the solvent coordination to the central metal of the porphyrin.
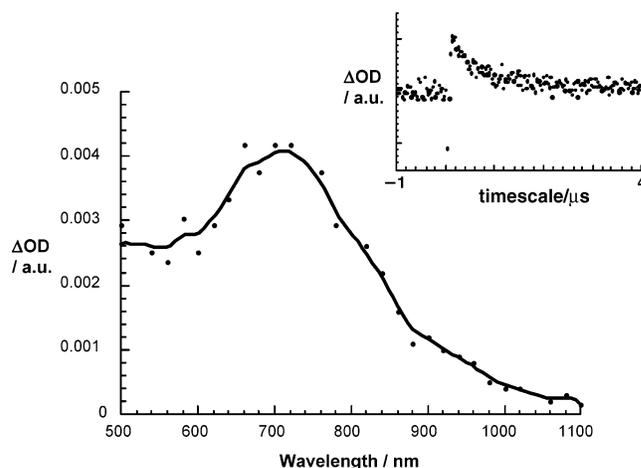

Figure 9. Nanosecond transient absorption spectrum (visible−near-infrared part) recorded with a 50 ns upon flash photolysis of dyad **Co3** (∼5.0 × 10^{-5} M) at 532 nm in deoxygenated anisole, indicating the Co(II)P π-radical cation features (λ_{max} = 680 nm) and C$_{60}$ π-radical anion features (λ_{max} = 900 nm) − Co(II)P$^{\bullet+}$−C$_{60}$$^{\bullet-}$. Insert depicts the decay of the Co(II)P π-radical cation features at 680 nm.
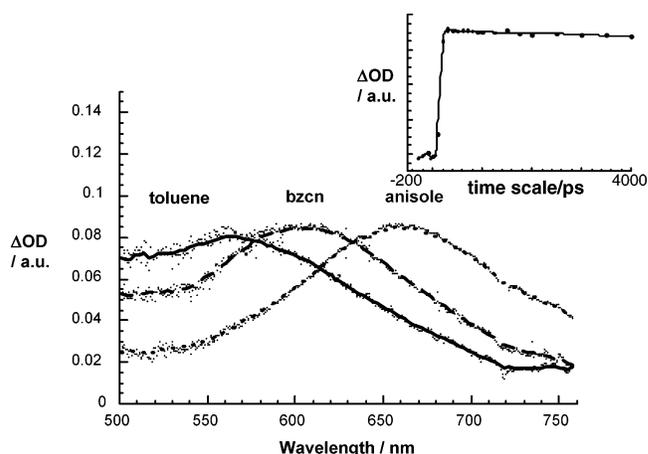

Figure 10. Picosecond transient absorption spectrum (visible part) recorded with a 100 ps upon flash photolysis of dyad **Co3** (∼5.0 × 10^{-5} M) at 532 nm in deoxygenated toluene (λ_{max} = 565 nm), benzonitirle (λ_{max} = 605 nm), and anisole (λ_{max} = 660 nm), indicating the Co(II)P π-radical cation features −Co(II)P$^{\bullet+}$. Insert depicts the stability of the Co(II)P π-radical cation features in anisole at 660 nm.

A reference experiment with toluene helped to shed light onto the electron-transfer aspect. In this aromatic solvent, we found spectroscopic evidence for **Co(II)P$^{\bullet+}$−C$_{60}$$^{\bullet-}$**. Likewise, in benzene and anisole the long-lived photoproduct, with lifetimes close to 1 μs, showed the characteristic marker of the **Co(II)P$^{\bullet+}$**. The nanosecond spectrum (i.e., recorded with a time delay of 100 ns) for **Co3** in anisole is depicted in Figure 9. Common to all these solvents is their aromatic character. Interestingly, the **Co(II)P$^{\bullet+}$** band is sensitively effected by the solvent, with peaks at 565 nm (toluene), 605 nm (benzonitrile), and 660 nm (anisole) (Figure 10). This trend suggests that the polarizability of the solvent plays a key role in determining the electron-transfer pathway. Since the ground-state absorption spectra reveal a notable perturbation of the electron density, namely, charges are moved, at least partially, from the electron donor (i.e., **Co(II)P**) to the electron acceptor (i.e., **C$_{60}$**), an electron deficient porphyrin is left behind. In the case of π-electron rich solvents, individual solvent molecules may undergo a type of π-stacking with the porphyrin chromophore.

Once this kind of complex is formed and a photoinduced electron transfer transfers the charges completely to the C_{60} core, where the electron is adequately delocalized, the positive charge can now be delocalized over the entire porphyrin macrocycle, extending into those solvent molecules that form the π-stacked complex. Consequently, charge separation lifetimes on the order of microseconds are noted, *3 orders of magnitude longer* than that seen for **Co(III)P−C$_{60}$$^{•−}$**.

In addition, complementary studies were performed with cyclohexanecarbonitrile and *o*-dichlorobenzene/*p*-nitrobenzene as solvents. In cyclohexanecarbonitrile, the nonaromatic analogue of benzonitrile, we found, not unexpectedly, the short-lived **Co(III)P−C$_{60}$$^{•−}$** state. Similarly, however, in *o*-dichlorobenzene and *p*-nitrobenzene, spectroscopic evidence also points to the formation of **Co(III)P−C$_{60}$$^{•−}$**. The radical pair lifetimes are between 0.4 and 0.21 ns. The discrepancy between the aromatic solvents raises the question if next to their comparatively high polarizabilities favoring $\pi−\pi$-stacking interactions with the porphyrin chromophore additional parameters might be operative and that influence the preferred formation of **Co(II)P$^{•+}$−C$_{60}$$^{•−}$** versus **Co(III)P−C$_{60}$$^{•−}$**. Steric effects, for example, should be considered, which we tested with *tert*-butylbenzene. Since this case also yielded the short-lived **Co(III)P−C$_{60}$$^{•−}$** state, we conclude tentatively that a complicated interplay between polarizability, steric bulk, and probably additional effects is responsible for this rather unusual behavior.

The lifetimes of the charge-separated states (i.e., **Co(III)P−C$_{60}$$^{•−}$**) can be correlated for **Co3** with the solvent polarity. The dependence of k_{CR} ($\tau = 1/k_{CR}$) versus free energy changes indicates stabilizing effects for the charge-separated state at higher $-\Delta G_{CR}°$ values. These are clear attributes of the "Marcus-inverted" region, the highly exergonic region ($-\Delta G°$ > λ), where the electron-transfer rates start to decrease with increasing free energy changes.[29] To add another low-polarity data point, we studied chloroform and found a lifetime for **Co(III)P−C$_{60}$$^{•−}$** of 1.1 ns. To quantify the driving force dependence on the rate constants (k_{CR}), the semiclassical Marcus equation was employed. From the best fits of the driving force dependence on charge recombination rates, the following values for the reorganization energies (λ) and electronic couplings (V) were derived: $\lambda = 0.84$ eV and $V = 18$ cm^{-1}. Please note that the electronic coupling element is substantially smaller than that in the **ZnP$^{•+}$−C$_{60}$$^{•−}$** case, where a similar analysis yielded a V value of 313 cm^{-1}. To confirm the small electronic coupling element, we transferred the semiclassical Marcus equation into a linear expression, eq 1.

$$k_{B}T \ln k_{ET} + \frac{\Delta G_{ET}°}{2} = k_{B}T \ln\left[\left(\frac{4\pi^3}{h^2\lambda k_{B}T}\right)^{1/2} V^2\right] - \frac{\lambda}{4} - \frac{(\Delta G_{ET}°)^2}{4\lambda} \quad (1)$$

A plot of [$k_{B}T \ln k_{BET} + (\Delta G_{BET}°/2)$] versus $(\Delta G_{BET}°)^2$ gave a linear correlation, as shown in Figure 11. Analysis of this plot afforded a reorganization energy of 0.75 eV and an electronic coupling of 15 cm^{-1}.
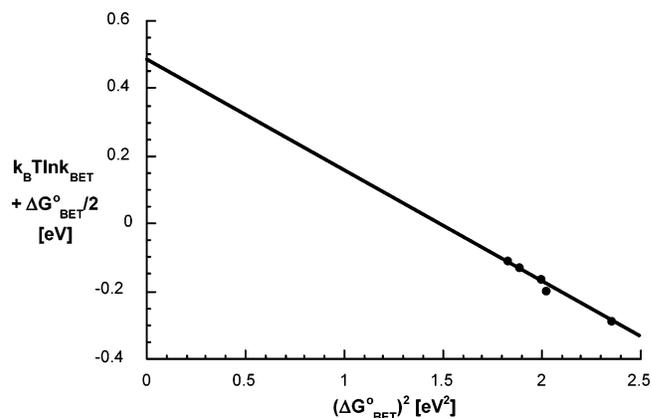

Figure 11. Plot of [$k_{B}T \ln k_{BET} + (\Delta G_{BET}°/2)$] versus $(\Delta G_{BET}°)^2$ for dyad **Co3**.

Now we turn to **Co1**. Because of the flexibility, which is associated with the donor−acceptor connection in **Co1**, different structural conformers are likely to be present in solution. An important aspect in control over orientation and structure are charge-transfer interactions, as they may prevail between the donor and acceptor moieties. Earlier we proposed that electron transfer in flexible dyads involves generation of a photoexcited intramolecular exciplex.[30] Formation of this critical intermediate takes typically several hundred of picoseconds. Considering the short-lived nature of photoexcited cobalt(II) porphyrins (i.e., less than 30 ps), an intramolecular electron transfer evolving from the latter is rather unfeasible. In line with this assumption, 532-nm excitation resulted only in the typical porphyrin deactivation. About 50 ps after the laser pulse the spectrum disappeared completely.

An alternative approach to initiate an electron transfer in **Co1** is the utilization of the fullerene excited states. In fact, the singlet (1.76 eV) and triplet (1.5 eV) excited states of C_{60} derivatives are both powerful oxidants[4f] to form either **Co(II)P$^{•+}$−C$_{60}$$^{•−}$** or **Co(III)P−C$_{60}$$^{•−}$** for which we determined energies around 1.4−1.3 eV. The well-known excited-state properties of methanofullerenes shall be discussed first, since they emerge as reference points for the interpretation of the features expected upon 355-nm illumination of dyad **Co1**. The singlet excited state, displaying a distinctive singlet−singlet transition around 900 nm, undergoes a quantitative intersystem crossing (ISC) to yield the long-lived triplet manifold, for which maxima are noted at 360 and 720 nm.

Detecting the instantaneous grow-in (i.e., 18 ps) of the 900-nm absorption affirms the successful C_{60} excitation in **Co1**. Instead of seeing, however, the slow ISC dynamics, the singlet−singlet absorption decays in the presence of Co(II)P with accelerated dynamics. The singlet excited-state lifetimes, as they were determined from an average of first-order fits of the time-absorption profiles at various wavelengths (850−950 nm) are 310 ps (toluene), 230 ps (THF), and 130 ps (benzonitrile). Spectroscopically, the transient absorption changes, taken after the completion of the decay, bear close resemblance with those seen for **Co3**. In particular, we found distinctly different products in THF and benzonitrile. In THF, the new transients reveal strong maxima at 560 and 590 nm, which match those of the one-electron oxidized Co(III)P. On the other hand, in benzoni-

(29) (a) Marcus, R. A.; Sutin, N. *Biochim. Biophys. Acta* **1985**, *811*, 265. (b) Marcus, R. A. *Angew. Chem., Int. Ed. Engl.* **1993**, *32*, 1111; *Angew. Chem.* **1993**, *105*, 1161.

(30) Guldi, D. M.; Luo, C.; Swartz, A.; Scheloske, M.; Hirsch, A. *Chem. Commun.* **2001**, 1066−1067.
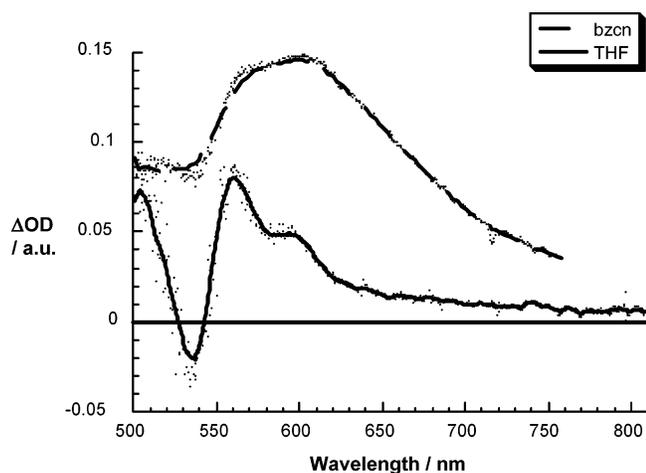
Figure 12. Picosecond transient absorption spectrum (visible part) recorded with a 100 ps upon flash photolysis of dyad **Co1** (3.0×10^{-5} M) at 532 nm in deoxygenated THF (solid line) and benzonitrile (dashed line).

trile the key feature of the new product is a broad maximum in the visible region around 600 nm, which resembles the one-electron oxidized Co(II)P π-radical cation, **Co(II)P$^{\bullet+}$**, seen in **Co3**. The spectral differences of the two spectra, namely, that of **Co(III)P** and that of **Co(II)P$^{\bullet+}$**, are illustrated in Figure 12. Concomitant with the **Co(III)P** and **Co(II)P$^{\bullet+}$** features in the visible, we noticed a near-infrared maximum at 1040 nm, corroborating the one-electron reduction of the electron accepting fullerene, **C$_{60}$$^{\bullet-}$**.

Thus, in flexible dyad **Co1**, formation of the radical pairs develops only as a result of the rapid decay of the fullerene singlet excited state, upon 355-nm excitation, while in dyad **Co3** even short-lived nature of photoexcited cobalt(II) porphyrins, which is less than 30 ps, was shown successfully to initiate an intramolecular electron transfer.

Conclusions

Compared to **Zn3** and *trans*-2 bisadduct **7** the first reduction of the fullerene moiety within **Co3** becomes easier by 40 mV in dichloromethane and 20 mV in benzonitrile, indicating significant interactions between the π-system of the fullerene and the d orbitals of the central Co atom. Comparison of the first oxidation step of the cobalt complexes (i.e., **9**, **Co4**, and **Co1**) reveals an interesting trend. Whereas in dichloromethane the first oxidation occurs at similar potentials ($+0.35 \pm 0.05$ V), in benzonitrile the first oxidation occurs at about 0.00 ± 0.05 V, except for **Co3**, whose potential is much more positive ($+0.28$ V). Such a large potential shift to positive potentials denotes in benzonitrile a destabilization of the cobalt(III) oxidation state in **Co3** compared to all other studied cobalt porphyrins and therefore a stabilization of the radical cation character. All these trends, as well as the peculiar behavior observed by spectroelectrochemistry for the first oxidation step of **Co3**, are in agreement with the generation of a cobalt(II) radical cation. Such a behavior has never been observed previously and is in agreement with the photophysical results observed in benzonitrile.

In photoinduced electron-transfer experiments, two different oxidation products were found besides **C$_{60}$$^{\bullet-}$** in the radical ion pair state, that is, either a metal-centered **Co(III)P** or a ligand-centered **Co(II)P$^{\bullet+}$**. In light of the drastic changes in photore-

activity, that is, formation of **Co(III)P$-$C$_{60}$$^{\bullet-}$** or **Co(II)P$^{\bullet+}$$-C_{60}$$^{\bullet-}$**, the aromatic character of the solvent certainly plays the major role. Appreciable π-stacking with the porphyrin chromophore is the overall driving force for stabilizing the long-lived **Co(II)P$^{\bullet+}$$-C_{60}$$^{\bullet-}$** state. But polarizability of the solvent is not the sole nature of the stacking. At this stage, it is evident that a combination of steric and other effects also contributes to the facilitation of this interesting phenomenon. Importantly, depending on the nature of the oxidation, that is, metal- versus ligand-centered process, charge recombination can be suppressed by up to *3 orders of magnitude*, reaching almost into the microsecond time domain. Considering the close donor$-$acceptor separation, namely, van der Waals contacts, the lifetimes are promising, although not comparable to previous findings, where separations are as large as 50 Å.[6b]

Experimental Section

Synthesis Protocols and Spectroscopic Data. Chemicals. C$_{60}$ was obtained from Hoechst AG/Aventis and separated from higher fullerenes by a plug filtration.[31,32] All analytical reagent-grade solvents were purified by distillation.[33] *trans*-2$-$C$_{62}$(COOEt)$_4$ (**7**),[13] ZnTPP (**8**),[2] CoT*t*-BuPP (**9**),[23] and **Zn3**[9a] were synthesized according to literature procedures in ref 4a.

Thin-Layer Chromatography (TLC). Riedel-de-Haën silica gel F$_{254}$ and Merck silica gel 60 F$_{254}$. Detection: UV lamp, H$_3$[P(Mo$_3$O$_{10}$)$_4$]/Ce(SO$_4$)$_2$/H$_2$SO$_4$/H$_2$O bath, KMnO$_4$/H$_2$O and iodine chamber.

Flash Chromatography (FC). ICN Silica 32$-$63, 60 Å; typical parameters for column diameter, loading, optimum eluant mixtures, eluant flow rate etc. were selected from the literature.[34]

High-Performance Liquid Chromatography (HPLC). Shimadzu liquid chromatograph LC-10AT with system controller SCL-10AVP, preparative liquid chromatographs LC-8A, diode array detector, auto injector, refractive index detector and UV/vis detector, selection valve, and fraction collector. Analytical columns: Nucleosil 5 μm, 200 $\times$ 4 mm, Macherey$-$Nagel; Gromsil 100 Si, NP1, 5 μm, 200 $\times$ 4 mm; Rexchrom Buckyclutcher 10 $\times$ 250 mm, Regis; and Nucleogel GFC 500-5, Macherey$-$Nagel. Preparative columns: Nucleosil 5 μm, 250 $\times$ 21 mm, Macherey$-$Nagel; Grom-Sil 100 Si, NP1, 5 μm, 250 $\times$ 20 mm; Nucleogel GFC 500-10, Macherey$-$Nagel; Buckyclutcher 250 $\times$ 21 mm.

NMR Spectra. JEOL JNM EX 400 and JEOL JNM GX 400 (^{1}H: 400 MHz, ^{13}C: 100.5 MHz), Bruker Avance 300 (^{1}H: 300 MHz, ^{13}C: 75,4 MHz), Bruker Avance 400 (^{1}H: 400 MHz, ^{13}C: 100.5 MHz). The chemical shifts are given in parts per million (ppm) relative to SiMe$_4$ (TMS). The resonance multiplicities are indicated as *s* (singlet), *d* (doublet), *t* (triplet), *q* (quartet), *m* (multiplet), and *br* (broad resonances).

UV/Vis Spectra. Shimadzu UV-3102 PC, UV$-$vis$-$NIR scanning spectrophotometer; absorption maxima λ_{max} are given in nanometers.

IR Spectra. Bruker FT-IR Vector 22, KBr pellets or thin film (NaCl plates), $\bar{\nu}$ values in cm^{-1}.

Mass Spectra. Micromass Zabspec, FAB (LSIMS) mode (3-nitrobenzyl alcohol) and ESI mode; Varian MAT 311A EI mode.

Porphyrins H$_2$4, H$_2$5, and H$_2$6. Typical Procedure. 3-(2-(Meth-oxymalonyloxy)ethoxybenzaldehyde (6.65 g, 25.0 mmol), benzaldehyde (2.53 cm^3, 25.0 mmol), pyrrole (3.48 cm^3, 50.0 mmol), and tetraphen-ylphosphonium chloride (58 mg, 0.15 mmol) were dissolved in CH$_2$-Cl$_2$ under N$_2$, and the solution was purged with N$_2$ for 10 min. Boron

(31) Reuther, U. Ph.D. Dissertation, University of Erlangen-Nürnberg, Germany, 2002.
(32) Isaacs, L.; Wehrsig, A.; Diederich, F. *Helv. Chim. Acta* **1993**, *76*, 1231.
(33) Perrin, D. D.; Amarego, W. L. F. *Purification of Laboratory Chemicals*, 3rd ed.; Pergamon Press: Oxford, 1988.
(34) Still, W. C.; Kahn, M.; Mitra, A. *J. Org. Chem.* **1978**, *43*, 2923$-$2925.

trifluoride etherate (630 μL, 5.0 mmol) was added, and the solution was stirred for 1 h under exclusion of light. *p*-Chloranil (9.25 g, 37.6 mmol) was then added, and the solution was heated at reflux for 1 h. The mixture was separated by multiple passage through flash chromatographic columns (SiO$_2$, CH$_2$Cl$_2$/EtOAc 20/1). The first porphyrin fraction contained tetraphenylporphyrin and was followed by monoester **H$_2$4**. The third and fourth bands contained bis-functionalized porphyrins **H$_2$6** and **H$_2$5**, respectively.

H$_2$4 (484 mg, 0.63 mmol, 5.0%): ^{1}H NMR (400 MHz, CDCl$_3$): δ = 8.84 (m, 8 H, β-C*H*), 8.21 (AA′BB′, 6 H, Ar*H*), 7.85 (d, 1 H, Ar*H*), 7.78 (s, 1 H, Ar*H*), 7.75 (m, 9 H, Ar*H*), 7.63 (t, 1 H, Ar*H*), 7.30 (d, 1 H, Ar*H*), 4.57 (t, ^3J = 4.64 Hz, 2 H, C*H*$_2$), 4.36 (t, ^3J = 4.64 Hz, 2 H, C*H*$_2$), 3.68 (s, 3 H, OC*H*$_3$), 3.44 (s, 2 H, CO−C*H*$_2$−CO), −2.57 (br. s, 2 H, N*H*). ^{13}C NMR (100.5 MHz, CDCl$_3$): δ = 166.76, 166.50 (*C*=O), 156.77, 143.63, 143.06, 142.13 (arom. *C*), 134.55 (arom. *C*H), 131.15 (β-*C*H), 128.17, 127.72, 127.61, 126.68, 121.12 (arom. *C*H), 120.28, 119.48, 118.73 (*meso-C*), 114.20 (arom. *C*H), 65.86, 63.85 (*C*H$_2$), 52.54 (O*C*H$_3$), 41.17 (CO−*C*H$_2$−CO). UV/vis (CH$_2$Cl$_2$): λ_{max}/ nm (lg ϵ) = 399 (sh, 4.87), 418 (5.65), 514 (4.21), 549 (3.77), 591 (3.63), 645 (3.42). MS (MALDI-TOF): m/z = 775 (MH$^+$). FT-IR (KBr): $\tilde{\nu}$/cm^{-1} = 3316, 3054, 3024, 2950, 1736, 1596, 1575, 1471, 1440, 1349, 1178, 1152, 964, 801, 730, 700.

H$_2$5 (449 mg, 0.48 mmol, 3.8%): ^{1}H NMR (400 MHz, CDCl$_3$): δ = 8.87 (m, 8 H, β-C*H*), 8.21 (AA′BB′, 4 H, Ar*H*), 7.85 (d, 2 H, Ar*H*), 7.79 (s, 2 H, Ar*H*), 7.72 (m, 6 H, Ar*H*), 7.60 (t, 2 H, Ar*H*), 7.28 (d, 2 H, Ar*H*), 4.52 (t, ^3J = 4.63 Hz, 4 H, C*H*$_2$), 4.31 (t, ^3J = 4.63 Hz, 4 H, C*H*$_2$), 3.65 (s, 6 H, OC*H*$_3$), 3.42 (s, 4 H, CO−C*H*$_2$−CO), −2.42 (br. s, 2 H, N*H*). ^{13}C NMR (100.5 MHz, CDCl$_3$): δ = 166.72, 166.45 (*C*=O), 156.73, 143.54, 142.04 (arom. *C*), 134.51 (arom. *C*H), 131.17 (β-*C*H), 128.12, 127.70, 127.59, 126.66, 121.12 (arom. *C*H), 120.32, 119.51 (*meso-C*), 114.12 (arom. *C*H), 65.78, 63.77 (*C*H$_2$), 52.48 (O*C*H$_3$), 41.10 (CO−*C*H$_2$−CO). UV/vis (CH$_2$Cl$_2$): λ_{max}/nm (lg ϵ) = 399 (sh, 4.82), 418 (5.58), 514 (4.16), 548 (3.79), 591 (3.66), 647 (3.49). MS (MALDI-TOF): m/z = 934 (MH$^+$); FT-IR (KBr): $\tilde{\nu}$/cm^{-1} = 3316, 3055, 3025, 2951, 2925, 2853, 1736, 1596, 1576, 1472, 1438, 1336, 1262, 1151, 964, 803, 733, 701.

H$_2$6 (227 mg, 0.24 mmol, 1.9%): ^{1}H NMR (400 MHz, CDCl$_3$): δ = 8.86 (m, 8 H, β-C*H*), 8.21 (AA′BB′, 4 H, Ar*H*), 7.78 (s, 2 H, Ar*H*), 7.75 (m, 6 H, Ar*H*), 7.62 (t, 2 H, Ar*H*), 7.28 (d, 2 H, Ar*H*), 4.55 (t, ^3J = 4.64 Hz, 4 H, C*H*$_2$), 4.34 (t, ^3J = 4.64 Hz, 4 H, C*H*$_2$), 3.68 (s, 6 H, OC*H*$_3$), 3.44 (s, 4 H, CO−C*H*$_2$-CO), −2.57 (br. s, 2 H, N*H*). ^{13}C NMR (100.5 MHz, CDCl$_3$): δ = 166.74, 166.47 (*C*=O), 156.77, 143.59, 142.08 (arom. *C*), 134.53 (arom. *C*H), 131.08 (β-*C*H), 128.16, 127.74, 127.63, 126.69, 121.14 (arom. *C*H), 120.25, 119.62 (*meso-C*), 114.20 (arom. *C*H), 65.86, 63.81 (*C*H$_2$), 52.52 (O*C*H$_3$), 41.16 (CO−*C*H$_2$−CO). UV/vis (CH$_2$Cl$_2$): λ_{max}/nm (lg ϵ) = 400 (sh, 4.90), 418 (5.65), 514 (4.26), 550 (3.85), 590 (3.74), 645 (3.58). MS (MALDI-TOF): m/z = 934 (MH$^+$). FT-IR (KBr): $\tilde{\nu}$/cm^{-1} = 3316, 3055, 3024, 2951, 2924, 2853, 1736, 1596, 1576, 1472, 1438, 1335, 1260, 1150, 972, 803, 733, 701.

5-{3-[3-(Methoxymalonyloxy)ethoxy]phenyl}-10,15,20-triphenylporphyrinato-cobalt(II) Co4. To a solution of 900 mg (1.9 mmol) of porphyrin **H$_2$4** in 200 cm^3 THF, 443 mg (1.8 mmol) Co(OAc)$_2$*4H$_2$O was added, and the mixture was heated for 3 h under reflux. The completing of the reaction was controlled by TLC. Subsequently, the solution was cautiously evaporated, and the residue was purified by flash-chromatography using an increasing solvent polarity gradient (silica, CH$_2$Cl$_2$/EtOAc 20:1 to 4:1).

Co4 (150 mg, 0.80 mmol, 10%): ^{1}H NMR (400 MHz, CDCl$_3$): δ = 3.63 (s, 3H, OC*H*$_3$), 3.66 (s, 2H, COC*H*$_2$CO), 5.11 (br, 2H, C*H*$_2$), 5.49 (br, 2H, C*H*$_2$), 9.32 (br, 1H, Ar*H*), 9.75 (br, 4H, Ar*H*), 9.95 (br, 6H, Ar*H*), 12.71 (br, 2H, Ar*H*), 13.11 (br, 6H, Ar*H*), 15.94 (br, 8H, β-C*H*). ^{13}C NMR (100.5 MHz): δ = 166.90 (*C*=O), 160.15, 158.29, 156.80, 141,13, 134.79, 131.47, 130.85, 130.27, 127.63, 117.33, 98.56 (arom. *C*), 67.13, 64.50 (*C*H$_2$), 53.04 (O*C*H$_3$), 41.31 (CO*C*H$_2$CO). UV/vis (CH$_2$Cl$_2$): λ_{max}/nm (log ϵ) = 346 (4.12), 405.5 (4.88), 532 (3.90).

MS (FAB, NBA): m/z = 832 [M$^+$]. FT-IR (KBr): $\tilde{\nu}$/cm^{-1} = 2964, 1734, 1684, 1647, 1637, 1596, 1575, 1541, 1508, 1488, 1348, 1309, 1261, 1191, 1178, 1146, 1103, 1069, 892, 794, 748, 714, 699.

1′-Methoxycarbonyl-1′-{2-[3-[5-[10,15,20-triphenylporphyrinato-cobalt(II)]]]-phenoxy}ethoxycarbonyl-1,2-methano[60]fulleren Co1. A mixture of 320 mg (0.385 mmol) of Co porphyrin **Co4**, 278 mg (0.385 mmol) of C$_{60}$, and 98 mg (0.385 mmol) of I$_2$ were dissolved in 200 cm^3 dry toluene under nitrogen protection, and subsequently 150 μL (1.04 mmol) of DBU was added. After being stirred for 48 h room temperature, the reaction solution was cautiously concentrated on a rotatory evaporater, and the residue was chromatographically purified by means of FC chromatography (silica, toluene/EtOAc 10:1). Pure **Co1** was obtained as an orange-colored substance.

Co1 (160 mg, 0.10 mmol, 26.8%): ^{1}H NMR (400 MHz, CDCl$_3$): δ = 3.80 (s, 3H, OC*H*$_3$), 5.04 (s, 2H, C*H*$_2$), 5.13 (s, 2H, C*H*$_2$), 8.70 (s, 1H, Ar*H*), 9.16−9.64 (m, 9H, Ar*H*), 10.10 (br, 1H, Ar*H*), 11.20−12.60 (br, 8H, Ar*H*), 14.70 (br, 8H, β-C*H*); ^{13}C NMR (100.5 MHz): δ = 162.19, 162.78 (*C*=O), 159.01, 141.69, 133.49, 130.20, 130.05, 129.55, 117.62 (arom. *C*), 68.53, 67.94 (C$_{60}$ sp^3), 65.18 (*C*H$_2$), 53.69 (O*C*H$_3$); UV/Vis (CH$_2$Cl$_2$): λ_{max}/nm (log ϵ) = 258 (5.01), 325 (4.62), 413.5 (4.82), 536.5 (3.96); MS (FAB, NBA): m/z = 1545 [M$^+$]; FT-IR (KBr): $\tilde{\nu}$/cm^{-1} = 1763, 1595, 1573, 1487, 1451, 1427, 1349, 1265, 1229, 1205, 1177, 1109, 1094, 1071, 1003, 956, 834, 796, 752, 700, 667, 580.

Metal-Free *trans*-2 Dyad H$_2$3. To a solution of 50 mg (0.030 mmol) of dyad **Zn3** in 25 mL of toluene, a 3% methanolic solution of trifluoroacetic acid was added. The reaction mixture was stirred at room temperature for 10 min. After being neutralized with aqueous NaHCO$_3$ solution and extracted with EtOAc, the organic layer was washed with H$_2$O, dried over Na$_2$SO$_4$, and concentrated in vacuo. A quantity of 48 mg (0.029 mmol, 96.6%) of the product was isolated by flash chromatography (silica, CH$_2$Cl$_2$/EtOAc 20:1).

^{1}H NMR (400 MHz, CDCl$_3$): δ = 8.71 (m, 8 H, β-C*H*), 8.27 (d, 2 H, Ar*H*), 8.17 (d, 2 H, Ar*H*), 7.96 (d, 2 H, Ar*H*), 7.80 (t, 2 H, Ar*H*), 7.71 (m, 8 H, Ar*H*), 7.39 (d, 2 H, Ar*H*), 5.17 (dt, ^3J = 5.50 Hz, 2 H, C*H*$_2$), 4.77 (dt, ^3J = 5.50 Hz, 2 H, C*H*$_2$), 4.52 (t, J = 5.50 Hz, 4 H, C*H*$_2$), 3.93 (s, 6 H, OC*H*$_3$), −3.00 (s, 2 H, N*H*). ^{13}C NMR (100.5 MHz, CDCl$_3$): δ = 163.63, 163.55 (*C*=O), 156.72 (arom. *C*), 147.75, 147.43, 145.66, 144.96, 144.93, 144.47, 144.15, 143.89 (fullerene sp^2 *C*), 143.67 (arom. *C*), 142.86, 142.71, 142.42, 142.30 (fullerene sp^2 *C*), 142.13 (arom. *C*), 141.95, 141.80, 141.63, 141.60, 141.51, 141.30, 141.09, 141.00, 140.90, 139.90, 139.69, 139.16, 138.32, 138.28, 137.99, 137.83 (fullerene sp^2 *C*), 134.33, 134.15 (arom. *C*H), 132.39 (β-*C*H), 127.85, 127.64, 126.92, 126.71, 126.58 (arom. *C*H), 120.43, 119.53 (*meso-C*), 115.36 (arom. *C*H), 70.69, 70.02 (fullerene sp^3 *C*), 67.33, 65.05 (*C*H$_2$), 53.85 (O*C*H$_3$), 49.09 (CO−*C*−CO). UV/vis (CH$_2$Cl$_2$): λ_{max}/nm (log ϵ) = 240 (5.05), 260 (5.07), 317 (4.67), 407 (sh, 4.77), 427 (5.34), 518 (4.09), 553 (3.75), 594 (3.64), 648 (3.40). MS (MALDI-TOF): m/z = 1652 (MH$^+$). FT-IR (KBr): $\tilde{\nu}$/cm^{-1} = 3057, 3023, 2951, 2922, 1752, 1597, 1575, 1472, 1434, 1238, 800, 729, 701, 527.

***Trans*-2 Dyad Co3.** **H$_2$3** (33 mg, 0.020 mmol) and Co(OAc)$_2$ (10 equiv) were dissolved in THF (10 cm^3) in a 25-cm^3 round-bottomed flask and heated to reflux with stirring under N$_2$ for 24 h, until TLC control (SiO$_2$, toluene/EtOAC 20:1) showed complete consumption of free base adduct starting material. The reaction mixture was concentrated on a rotary evaporator and filtered through a silica gel plug (CH$_2$-Cl$_2$). A dark brown solid was obtained upon evaporation and recrystallization (CH$_2$Cl$_2$/MeOH) of the colored product fraction.

(30 mg, 0.018 mmol, 88%): Found: C, 78.81; H, 2.36; N, 3.28% (C$_{116}$H$_{40}$CoN$_4$O$_{10}$: C, 81.55; H, 2.36; N, 3.28%): %. ^{1}H NMR (400 MHz, CS$_2$/CDCl$_3$): (paramagnetic!) δ = 14.77 (br. s, 8 H, β-C*H*), 12.94 (br. s, 2 H, Ar*H*), 12.47 (br. s, 2 H, Ar*H*), 11.26 (br. s, 2 H, Ar*H*), 9.81 (br. s, 2 H, Ar*H*), 9.56 (br. s, 2 H, Ar*H*), 9.24 (br. s, 6 H, Ar*H*), 8.85 (br. s, 2 H, Ar*H*), 5.21 (br. s, 4 H, C*H*$_2$), 5.00 (br. s, 4 H, C*H*$_2$), 3.62 (br. s, 6 H, OC*H*$_3$). UV/vis (CH$_2$Cl$_2$): λ_{max}/nm (lg ϵ) = 262 (5.08), 319 (4.71), 419 (5.12), 530 (4.13). MS (FAB, NBA): m/z =

1707 (M^+), 720 (C_{60}^+). FT-IR (KBr): $\tilde{\nu}/cm^{-1}$ = 3450, 2955, 1751, 1600, 1578, 1433, 1352, 1262, 1240, 1178, 1109, 1075, 1006, 798, 702, 527.

Electrochemistry. All compounds were studied in CH_2Cl_2 + 0.1 M Bu_4NPF_6 and in benzonitrile + 0.1 M Bu_4NPF_6, respectively. The electrochemical measurements were carried out at room temperature (20 °C) in CH_2Cl_2 containing 0.1 M Bu_4NPF_6 in a classical three-electrode cell. The electrochemical cell was connected to a computerized multipurpose electrochemical device (Autolab, Eco Chemie BV, The Netherlands) controlled by a GPES software (v. 4.7) running on a PC computer. The working electrode was a glassy carbon (GC) disk electrode (diameter: 3 mm) used either motionless for cyclic voltammetry (ν =10 mV s^{-1} to 10 V s^{-1}) or as a rotating disk electrode.

The auxiliary electrode was a platinum wire, and the reference electrode was an aqueous Ag/AgCl/KCl (sat.) electrode. All potentials are referred to the ferrocene/ferrocenium (Fc^+/Fc) couple used as the internal standard. Under our experimental conditions, ferrocene was oxidized at +0.40 V versus Ag/AgCl. The accessible potential domain ranged from +1.4 to −2.4 V versus Fc^+/Fc. CH_2Cl_2 (Merck, spectroscopic grade) was dried over molecular sieves (4 Å) and stored under argon. Bu_4NPF_6 (Fluka, electrochemical grade) was used as received. The electrolyte was degassed by bubbling argon through the solution for at least 5 min, and an argon flow was kept over the solution during measurements.

Studies carried out in benzonitrile were made in a glovebox under drastic exclusion of water and oxygen (less than 2 ppm) as described elsewhere.[36] The classical three-electrode cell was connected to a Princeton Applied research potentiostat 263, controlled by a Powerlab/Echem electrochemical system (ADInstruments, USA). The working electrode was a platinum disk (2 mm in diameter), the auxiliary electrode a platinum wire, and the pseudo reference electrode was also a platinum wire. Ferrocene, used as an internal standard, was introduced to the solution at the end of the study. All given potentials are therefore given versus ferrocene in agreement with the IUPAC recommendation.[37] Spectroelectrochemical experiments were carried out as described elsewhere.[36]

Photochemistry. Picosecond laser flash photolysis experiments were carried out with 532-nm laser pulses from a mode-locked, Q-switched Quantel YG-501 DP Nd:YAG laser system (pulse width 18 ps, 2−3 mJ/pulse). Nanosecond laser flash photolysis experiments were performed with laser pulses from a Quanta-Ray CDR Nd:YAG system (532 nm, 6 ns pulse width) in a front face excitation geometry. The photomultiplier output was digitized with a Tektronix 7912 AD programmable digitizer. Fluorescence lifetimes were measured with a laser strope fluorescence lifetime spectrometer (Photon Technology International) with 337-nm laser pulses from a nitrogen laser fiber-coupled to a lens-based T-formal sample compartment equipped with a stroboscopic detector. Details of the laser strobe systems are described on the manufacturer's web site, http://www.pti-nj.com. Emission spectra were recorded with a SLM 8100 spectrofluorometer. The experiments were performed at room temperature. A 570-nm long-pass filter in the emission path was used to eliminate the interference from the solvent and stray light for recording the fullerene fluorescence. Each spectrum was an average of at least five individual scans and was corrected by using the correction function supplied by the manufacturer, by subtraction of the photomultiplier dark counts signal.

Supporting Information Available: Picosecond transient absorption spectrum recorded with a 100 ps flash photolysis of dyad **Zn3**. This material is available free of charge via the Internet at http://pubs.acs.org.

JA048983D

(35) Hashino, M.; Sonoki, H.; Miyazaki, Y.; Iimura, Y.; Yamamoto, K. *Inorg. Chem.* **2000**, *39*, 4850.
(36) Bley-Escrish, J.; Gisselbrecht, J. P.; Vogel, E.; Gross, M. *Eur. J. Inorg. Chem.* **2002**, 2829−2837.
(37) Gritzner, G.; Kuta, J. *Pure Appl. Chem.* **1984**, *56*, 461−466.
(38) Guldi, D. M.; Imahori, H.; Tamaki, K.; Kashiwagi, Y.; Yamada, H.; Sakata, Y.; Fukuzumi, S. *J. Phys. Chem.* **2004**, *108*, 541−548.